Comparative Analysis of Energy Yield between PERC and HJT Modules Tested in Experimental Campaigns Carried out in Northern Italy

Gabriele Malgaroli *Dip. Energia "Galileo Ferraris"*
Politecnico di Torino
Turin, Italy
gabriele.malgaroli@polito.it
Alessandro Ciocia *Dip. Energia "Galileo Ferraris"*
Politecnico di Torino
Turin, Italy
alessandro.ciocia@polito.it
Filippo Spertino *Dip. Energia "Galileo Ferraris"*
Politecnico di Torino
Turin, Italy
filippo.spertino@polito.it

Silvia Casagrande *Research, Development & Technological Innovation Dept.*
Edison Spa
Turin, Italy
silvia.casagrande@edison.it Luca Saglietti *Research, Development & Technological Innovation Dept.*
Edison Spa
Turin, Italy
luca.saglietti@edison.it

Abstract

The heterojunction (HJT) solar cells based on the integration of monocrystalline silicon and amorphous crystalline layers provide a remarkable improvement in terms of efficiency with respect to the Passivated Emitter and Rear Cell (PERC) modules, which are currently installed in most of plants. However, the efficiency gain in terms of energy production is not estimated by recent works in literature for the Mediterranean area: hence, this paper presents a comparative study of energy yield in Torino (latitude of 45° North, Italy) between PERC and HJT modules currently available on the market for conventional PhotoVoltaic (PV) installations, having rated power higher than 400 W. The modules were tested in experimental campaigns taking place in 2023 from April to September. In particular, this work quantifies the real energy yield improvements of HJTs with respect to PERC PV modules, resulting in an energy gain of HJTs between 3% and 6%. Finally, the dependence of these energy yield gains on irradiance and modules' temperature is investigated.

Index Terms

passivated emitter and rear cell; PERC; heterojunction; HJT; high-efficiency, energy yield.

I. Introduction

In the last decades, the global energy demand has significantly raised due to events like the population growth and the increased urbanisation. In this context, the exploitation of Renewable Energy Systems (RES) has been fundamental to fulfil the energy consumption by emitting low polluting emissions. The most diffused RESs are solar PhotoVoltaic (PV) plants and wind farms. Actually, according to the International Energy Agency, the new installations in 2023 of these systems were 95% of RES plants [1] and this ratio is expected to be constant until 2028.

Regarding wind farms, one field of research consists of evaluating their real performance and comparing experimental data recorded by Supervisory Control And Data Acquisition (SCADA) instruments with manufacturer specifications [2]. On the contrary, researchers in the PV field are working in areas of study including the development of models to predict PV performance under unconventional operating conditions, e.g. under electrical mismatch [3]; or the manufacturing of new high-performance materials to increase the conversion efficiency of PV modules [4].

Actually, for decades, most of PV modules production was based on the old aluminum back surface field (Al-BSF) technology [5], which provided moderate conversion efficiencies lower than 20% but its manufacturing process was simple and reliable [6]. Currently, the crystalline silicon (c-Si) technology is the most diffused, with a market share higher than 97

%. However, the diffusion of more efficient technologies in cell designs is increasing. In this context, the Passivated Emitter and Rear Cell (PERC) technology [7] was the first major improvement permitting module efficiencies up to 22% [8] with a manufacturing process not far from that of Al-BSF. Other approaches are the all back-contact, the interdigitated back contact, and the heterojunction technologies, with a joint market share lower than 10% in 2022 [9]. Such modules provide the highest performance, with conversion efficiency up to about 24%; however, their cost is significantly higher than PERC and Al-BSF, and their manufacturing requires substantial changes. In the recent years, industrial interest on HJT has renewed and their installations are increasing thanks to their higher expected performance and decreasing cost.

Nevertheless, researchers are exploring the possibility to integrate HJT cells with other high performance materials, like perovskite. In this case, the goal is to produce tandem PV modules with efficiencies higher than 30% by exploiting the different conversion spectrum [4] of c-Si and perovskite cells. In the literature, a very few papers evaluate the real efficiency gain of HJT with respect to PERC modules: for example, [10] and [11] compare different PV technologies in temperate climatic conditions (Milan, Italy, and Perth, Australia) by analysing old PV modules, with rated power $<< 300$W. The paper [12] analyzes the performance of modules based on the old and less efficient thin film technology in Malaga (Spain). Finally, the work [13] presents an experimental study on the energy yield performance of different PV technologies in China. However, the results might be significantly different for recent modules with actual technologies or in locations with different latitude or climate conditions, such as Mediterranean countries.

This paper presents a comparative analysis of energy yield between PERC and HJT modules that are currently available for residential installations. The modules under test were subject to outdoor experimental campaigns carried out in 2023 from April to September in Torino (Italy), have the same active surface, a rated power of 410 W (PERC) and 435 W (HJT), and a conversion efficiency of 21% (PERC) and 22% (HJT). Finally, this work evaluates the effect of weather conditions like irradiance and modules' temperature on the energy yield gain.

The paper is structured as follows: Section II presents the most important features of the technologies the modules under test belong to. Section III presents the measurement station used to carry out the experimental campaigns, and Section IV describes the methodology adopted to analyze the data collected in the experimental campaigns. Section V presents the specifications of the PV modules under test as well as the testing protocols. Section VI includes the results of the analysis, and Section VII contains the conclusions.

II. PERC vs. HJT Technologies

This section shortly presents the most important features of PERC and HJT technologies, higlighting their differences.

A. Passivated Emitter and Rear Surface (PERC) technology

These modules have a passivation layer on the rear of their cells, tyically made of materials like SiO_2, Al_2O_3 or SiN_x, which require manufacturing processes at high temperatures ($> 900°C$). This layer permits to reduce recombination losses thanks to an increased energy gap, and increase light absorption with respect to Al-BSF technology. A capping layer made of a-Si:H is, generally, placed above the passivation layer to reduce its degradation over time [6]. As a result, the generated voltage of each PERC cell is higher than that of Al-BSF, with common values of about 0.66 eV [14], and the temperature coefficient for maximum power is $< -0.5\%/°C$ in absolute value. The highest achieved efficiency was slightly lower than 24.5% for PERC cells [15].

B. Heterojunction (HJT) technology

HJT cells consist of an n-type c-Si wafer coated on both sides with thin intrinsic and doped amorphous silicon (a-Si) layers (having a thickness of a few nanometres) to minimize surface recombination and prevent defect generation [16]. At the top of HJT cell, an additional layer named Transparent Conductive Oxide (TCO) acts like a reflective layer, leading the carries to the electrode. With respect to PERC modules, in the HJTs, the a-Si layer absorbs the photons in a different wavelength range than c-Si, permitting to furtherly increase the efficiency up to values slightly lower than 27% at cell level [17], [18]. In addition, the generated voltage of each HJT cell is about 0.7 eV, and the temperature performance is significantly better than PERC, with a temperature coefficient for maximum power $< -0.3\%/°C$ in absolute value [19].

III. Description of the Acquisition System

The outdoor measurement station of Edison spa was used to carry out the experimental campaigns under analysis. This station was installed on the roof of the Energy Center building (Torino, Italy) under the supervision of the Energy Department from Politecnico di Torino. In particular, the measurement station consists of the following components:

- two programmable electronic loads with maximum power of 800 W, resolution of 16 bits, and relative uncertainty lower than $\pm 0.25\%$ (current) and $\pm 0.15\%$ (voltage). The electronic loads behave as resistors with variable resistance and each one was connected to one of the PV modules under test. In particular, the electronic loads include an algorithm to identify the maximum power point of the PV modules: this is achieved by scanning the power-voltage curve of the module from

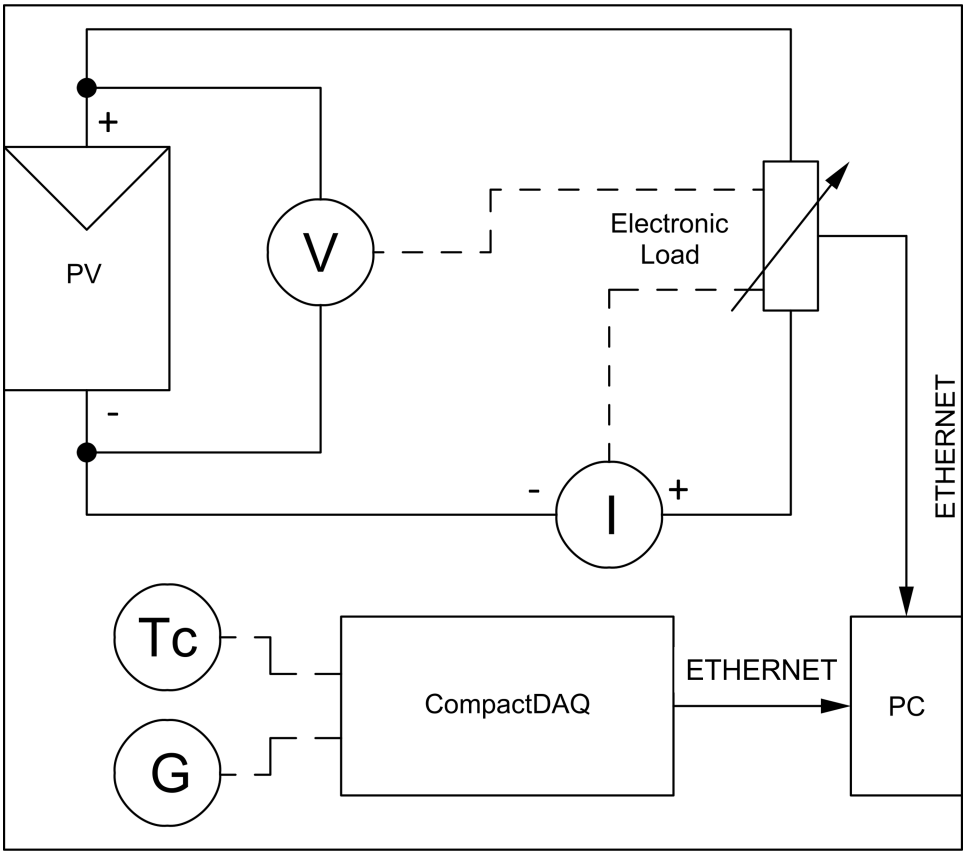

Fig. 1. Scheme of the measurement circuit for PV modules under test.

short circuit to open circuit states with variable resistance levels. Hence, the electronic loads can maintain the operating condition of the PV modules close to their maximum power point, and acquire the electrical data (voltage and current);

- two PT100 sensors with resolution of 0.1 °C, and relative uncertainty $< \pm 0.3°C$. Each sensor is connected to one PV module to measure its rear temperature;
- one spectrally flat class A pyranometer (measurement range 0-2000 $\mathrm{W/m^2}$ and relative uncertainty of ± 20 $\mathrm{W/m^2}$) acquires the in-plane solar irradiance G;
- one weather station includes one anemometer to acquire the wind speed (resolution of 0.01 m/s and relative uncertainty of $\pm 1\%$) and its direction (resolution $0.1°$ and relative uncertainty of $\pm 1\%$), one piezoresistive sensor to acquire the atmospheric pressure (resolution of 0.1 mbar, relative uncertainty of ± 0.4 mbar), one PT100 sensor to measure the ambient temperature (resolution of $0.1°C$, relative uncertainty $< \pm 0.3°C$), and a capacitive sensor to measure the relative humidity (resolution of 0.1%, relative uncertainty of $\pm 2.5\%$).
- one personal computer runs the control software in LABVIEW ambient to store the electrical and environmental quantities in a dedicated database.

Fig. 1 shows the schematic of the measurement station.

IV. Methodology

The method used in this work to compare the energy yield of different technologies consists of five steps (flowchart in Fig. 2):

- *Step #1 - Selection of high irradiance measurements.*
  In this step, three *I-V*curves are selected at the beginning of the experimental campaign. These curves are used to compare the performance of the PV module sunder study with the specifications provided by the manufacturers. High irradiance conditions (higher than 900 $\mathrm{W/m^2}$) are suggested.
- *Step #2 - Correction of high irradiance measurements to STC.*
  The specifications of the PV modules in the datasheets are provided at Standard Test Conditions (STC, corresponding to irradiance G_{STC} = 1000 $\mathrm{W/m^2}$ and modules' temperature $T_{\mathrm{STC}} = 25°C$). However, under natural sunlight, these weather conditions are rarely met and the measured PV performance needs to be corrected to STC to be compared with the datasheets.

This correction was carried out by applying the following equations from the international standards [20] to the three high irradiance measurements previously selected, where the subscript "m" refers to measured quantities:

$$I_{\mathrm{STC}} = I_{\mathrm{m}} + I_{\mathrm{sc,m}} \cdot \left(\frac{G_{\mathrm{STC}}}{G_{\mathrm{m}}} - 1 \right) + \alpha \cdot (T_{\mathrm{STC}} - T_{\mathrm{m}}) \tag{1}$$

$$V_{\mathrm{STC}} = V_{\mathrm{m}} - R_{\mathrm{s,m}} \cdot (I_{\mathrm{STC}} - I_{\mathrm{m}}) - k \cdot I_{\mathrm{STC}} \cdot (T_{\mathrm{STC}} - T_{\mathrm{m}}) + \beta \cdot (T_{\mathrm{STC}} - T_{\mathrm{m}}) \tag{2}$$

The quantities of the equation are the following:

- I_{STC} is the current at STC conditions.
- I_{m} is the measured current.
- $I_{\mathrm{sc,m}}$ is the measured short circuit current.
- V_{STC} is the voltage at STC conditions.
- V_{m} is the measured voltage.
- $R_{\mathrm{s,m}}$ is the series resistance of the module.
- G_{m} is the measured irradiance.
- T_{m} is the measured temperature.
- α is the thermal coefficient of current.
- β is the thermal coefficient of voltage.
- k is a correction parameter.

- *Step #3 - Comparison with manufacturer specifications.*
  In this step, the average values of STC voltage at open circuit and at the maximum power point (V_{oc} and V_{MPP}, respectively), STC current at short circuit and at the maximum power point (I_{sc} and I_{MPP}, respectively), maximum power and rated efficiency at STC (P_{nom} and η_{STC}) are evaluated between the three high irradiance measurements of each PV module. Then, the relative deviations of each quantity with respect to the values in the datasheets (ΔP, ΔV_{oc}, ΔV_{MPP}, ΔI_{sc}, ΔI_{MPP}) are computed as the ratio between the absolute deviations and the quantity from the datasheets.
- *Step #4 - Evaluation of energy yield for each module under test.*
  In this step, the total energy yield is computed for each PV module by integrating the power measurements over the time of the experimental campaign.
- *Step #5 - Energy yield deviations as functions of weather conditions.*
  In this step, the energy yield deviations among the technologies under study are presented as functions of irradiance and modules temperature. This operation permits to identify the conditions more favourable for the different devices under test.

V. Modules under Test and Testing Protocols

A. Modules under Test

The PV modules under test are four: two identical PERC modules and two identical HJTs. The modules were tested two at a time (one PERC and one HJT at a time) and they were subject to two experimental campaigns (2 months-duration each) carried out between the end of April and the end of June, and one carried out between the end of June and the end of September. The modules under test had South orientation and inclination of 30° with respect to the horizontal plane. Their electrical specifications are reported in Table I. A picture of the modules is presented in Fig. V.

TABLE I
Manufacturer Parameters of PV Modules under Test.

	PERC (#1)	HJT (#2)
$P_{\mathbf{nom}}$	410 W	430 W
$\eta_{\mathbf{STC}}$	21%	22%
$V_{\mathbf{oc}}$	37.32 V	40.1 V
$I_{\mathbf{sc}}$	13.95 A	13.38 A
$V_{\mathbf{MPP}}$	31.45 V	33.8 V
$I_{\mathbf{MPP}}$	13.04 A	12.76 A
α	+0.045%/°C	+0.04%/°C
β	-0.275%/°C	-0.24%/°C
γ	-0.35%/°C	-0.26%/°C
Power tolerance	(-3%, +3%)	(-3%, +3%)

B. Testing Protocols

The experimental campaigns carried out followed the indications by the International Energy Agency regarding the energy yield estimation tests for a specific site over a long period [21]. Actually, the tests were based on the repetition over a cycle

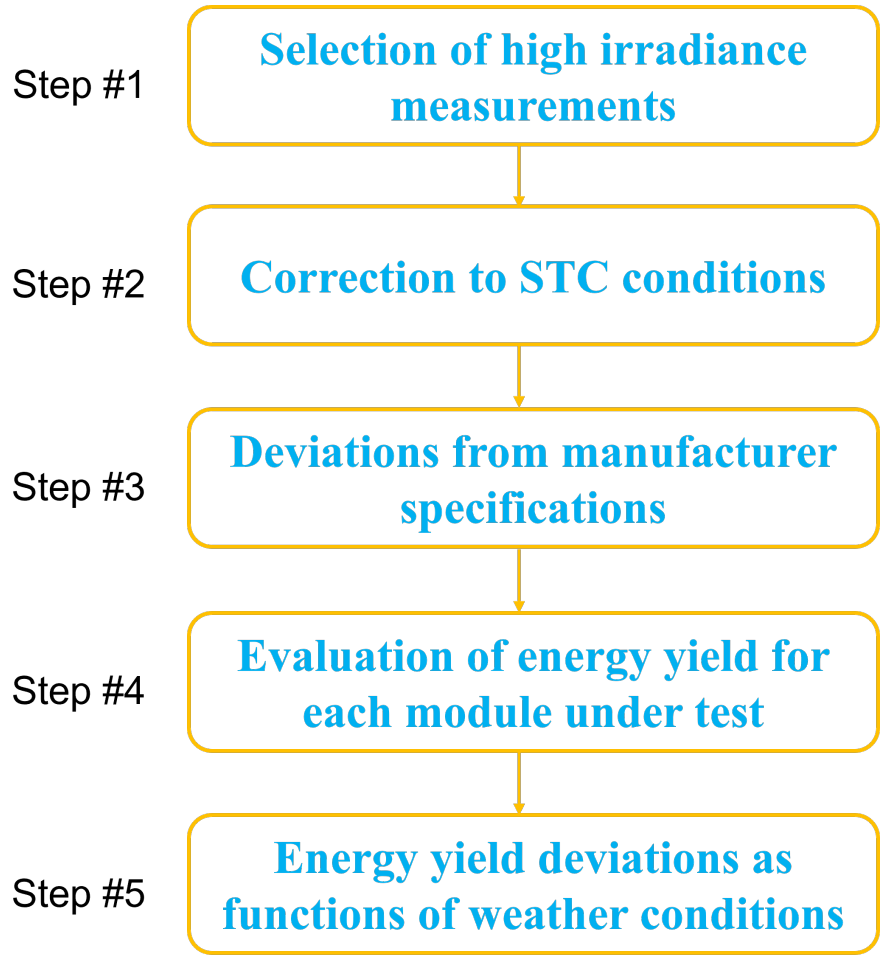

Fig. 2. Method used in the present analysis.

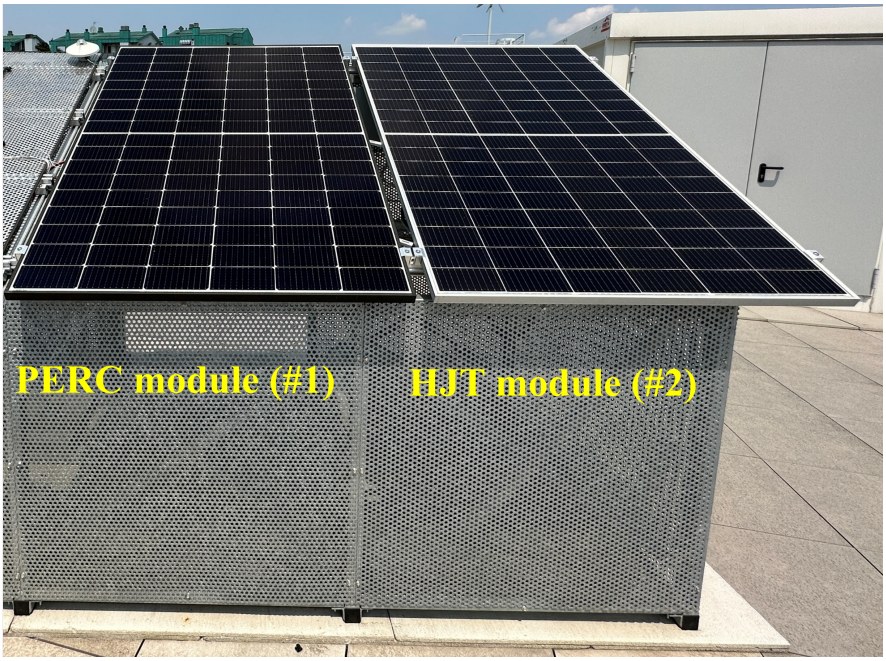

Fig. 3. Modules under test: PERC on the left and HJT on the right.

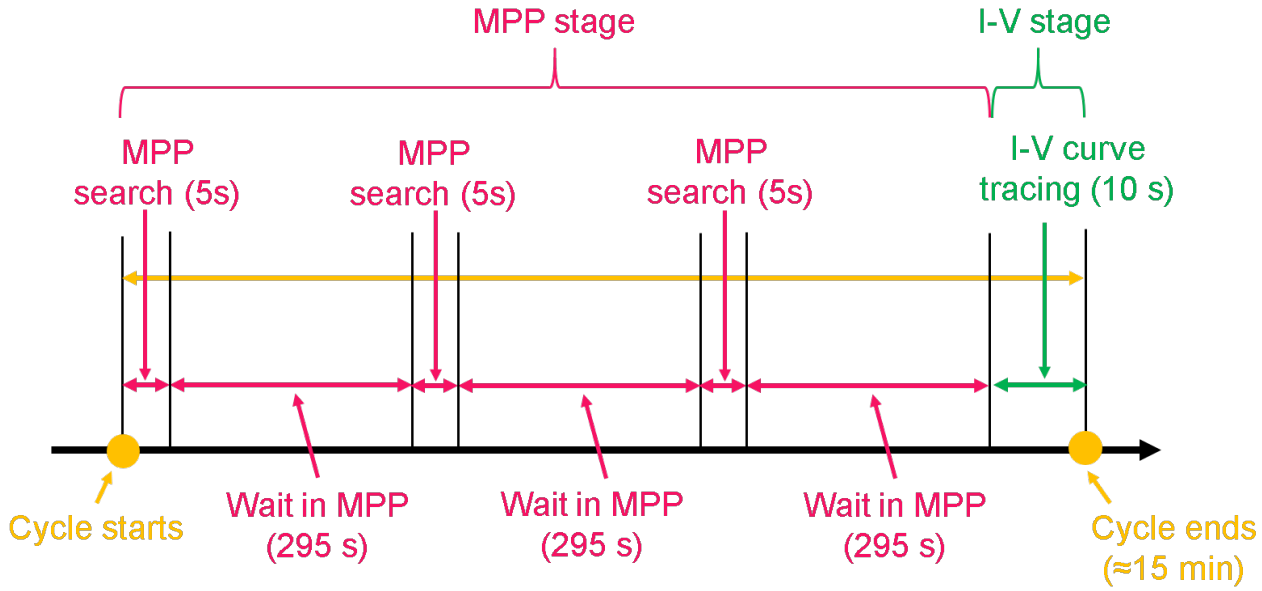

Fig. 4. Testing protocol used in the experimental campaigns.

consisting of two stages: the MPP and the I-V curve phases for the energy yield test. Their duration was equal to 15 min and 10 s, respectively. The main characteristics of these stages were the following:

- The MPP stage consisted of three MPP searches (duration of 5 s each) that were performed by imposing a variable voltage to the modules. Actually, the entire curves of the modules were scanned sweeping the entire *I-V*curve from the open-circuit to the short-circuit state. In this operation, the electronic load behaved like a resistor with variable resistance between almost zero (short-circuit) and infinite (open-circuit), and each operating condition was obtained by modifying the resistance value.
- After the identification of the maximum power point in each MPP search, the modules were maintained at their operating point for 295 s.
- After the MPP stage, the *I-V*curves of the modules were determined with the same principle of the MPP stage. The duration of each *I-V*curve tracing was 10 seconds.

Fig. 4 presents the different stages of a cycle, as well as the durations of each substage.

VI. Results

At the beginning of each experimental campaign, the performance of each module in three high irradiance conditions was selected (step #1) and corrected to Standard Test Conditions (step #2) using equations (1) and (2). The average STC performance of the four modules (step #3) is reported in Table II. Considering the power tolerance by the manufacturer (-3% - +3%), and the additional uncertainty of the measurement system (about $\pm 3\%$), the deviations from the manufacturers' specifications are within the margin of tolerance. However, it is relevant observing that the power deviations ΔP are mainly due to current deviations ΔI_{MPP} rather than voltage deviations ΔV_{MPP} at the maximum power point. Fig. 5 presents the *I-V*curves corrected to STC for the PERC and HJT modules measured in the 1^{st} day of the 1^{st} campaign.

The energy yield of the PV modules was computed by assuming PV power recorded in each MPP stage to be constant over the duration of each MPP substep (5 min). In addition, the power measured during the *I-V*stage was supposed constant over the *I-V*stage duration of 10 s. The resulting energy yield improvements ΔY were calculated as the ratio between the deviation of HJT yield Y_{HJT} with respect to that of PERC Y_{PERC}, and Y_{PERC}. This quantity was equal to +3.8% and +5.3% for the first and second experimental campaign, respectively. The energy yield improvements are mainly related to high irradiance and high temperature conditions. Fig. 6 and 7 present the power profiles of the modules for one typical clear sky day and one typical cloudy day, respectively. For these days, the daily yield increase corresponds to +5.6% (clear sky) and +3.2% (cloudy). These results are confirmed by the classification of energy yield improvements according to different irradiance and modules' temperature ranges, which is shown in Fig. 8 and 9 for the first campaign, and in Fig. 10 and 11 for the second campaign. The energy yield gain provided by HJT modules increases with sunny weather conditions. Actually, values up to about 6% and 8%, are observed for the first and second campaign, respectively, with irradiance close to 1000 W/m^2 and modules' temperature close to $70°C$. On the contrary, the energy gain becomes almost negligible at very low operating temperatures, being lower than 2% under low irradiance ($< 100\text{W}/\text{m}^2$).

TABLE II
ELECTRICAL PARAMETERS AT STC OF PV MODULES UNDER TEST.

	1st campaign		2nd campaign	
	PERC (#1)	HJT (#2)	PERC (#1)	HJT(#2)
$P_{\mathbf{nom}}$	395 W	413 W	397 W	416 W
$V_{\mathbf{oc}}$	38.05 V	40.71 V	38.07 V	40.68 V
$I_{\mathbf{sc}}$	12.96 A	12.32 A	13.10 A	12.44 A
$V_{\mathbf{MPP}}$	32.16 V	35.49 V	32.25 V	35.09 V
$I_{\mathbf{MPP}}$	12.27 A	11.64 A	12.30 A	11.86 A
$\eta_{\mathbf{STC}}$	20.2%	21.1 %	20.3%	21.3 %
ΔP	-3.7%	-4.0%	-3.3%	-3.2%
$\Delta V_{\mathbf{oc}}$	+1.9%	+1.5%	+2.0%	+1.5%
$\Delta I_{\mathbf{sc}}$	-7.1%	-7.9%	-6.1%	-7.0%
$\Delta V_{\mathbf{MPP}}$	+2.3%	+5.0%	+2.5%	+3.8%
$\Delta I_{\mathbf{MPP}}$	-5.9%	-8.8%	-5.6%	-7.1%

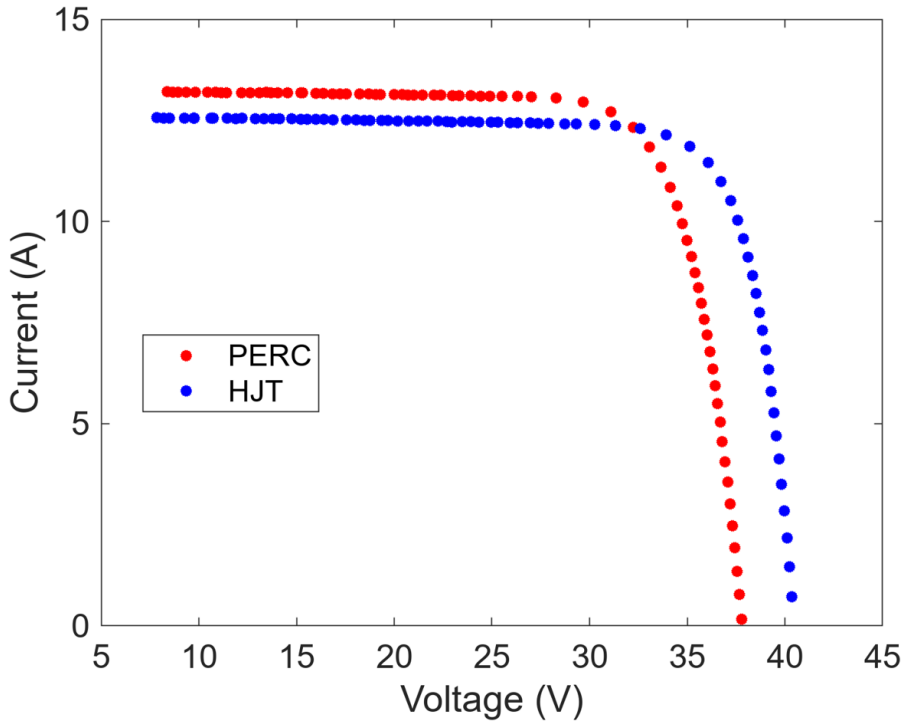

Fig. 5. *I-V*curves of PERC and HJT modules corrected to STC during the 1^{st} day of the 1^{st} campaign.

Achieving a complete uniformity while testing PV modules in different experimental campaigns is not possible. However, the performance of the modules after the STC correction were comparable between the campaigns. The weather conditions of experimental campaigns taking place in different months could be very different: in this work, the irradiance and modules' temperature ranges were comparable among the campaigns, as well as the irradiance frequency distribution. The most relevant difference was related to the frequency distribution of temperature values, which was shifted towards higher values in the second campaign. This factor confirms that the production gain by the heterojunction module was more evident in high temperature conditions, with a higher energy yield.

Currently, these considerations are valid for the period April - September in Italy after testing two PV modules per technology. These results will be extended in future works as experimental campaigns have begun to test a higher number of PV modules belonging to the same technology, increasing the statistics of the analysis.

VII. CONCLUSIONS

The Heterojunctions (HJTs) provide a remarkable efficiency improvement with respect to the Passivated Emitter and Rear Cell (PERC) modules, which are currently installed in most of residential plants. This paper presented a comparative study of energy yield between PERC and HJT modules currently available on the market. Four PV modules (two for each technology) were tested in two experimental campaigns carried out in 2023 from April to September in Torino (latitude of 45° North, Italy). The energy efficiency gain was +3.8% and +5.3% for the first and second experimental campaign, respectively. Such gains mainly occurred for high temperature-high irradiance conditions as they reached the maximum value (about +6% and +8%

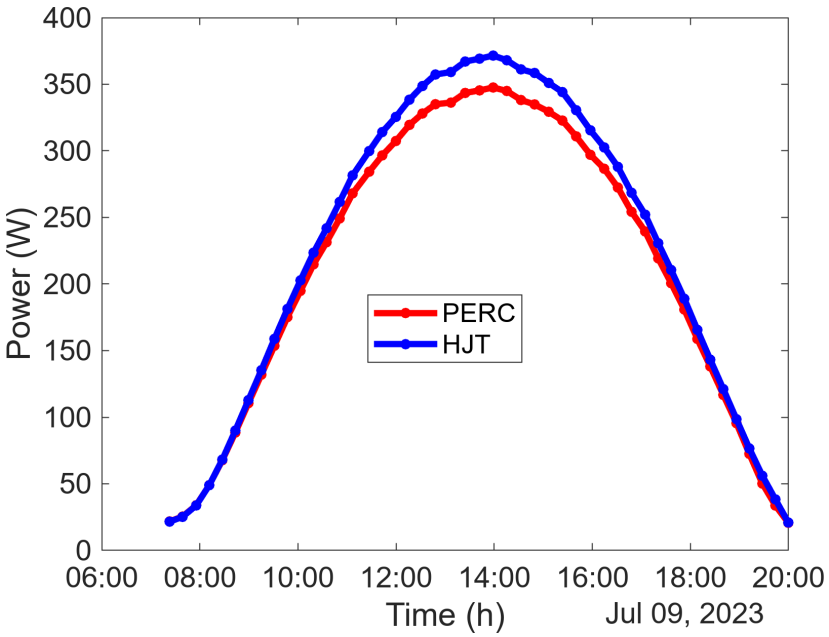

Fig. 6. Power profiles of PERC and HJT modules during a clear sky day.

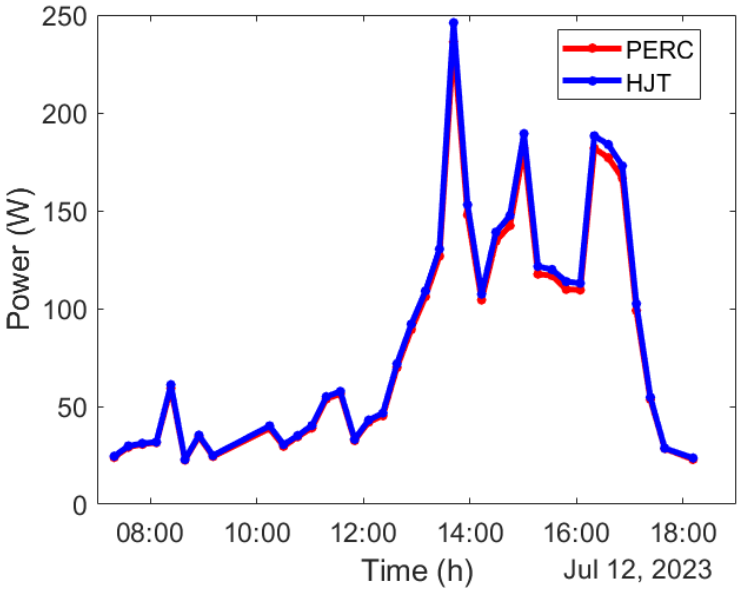

Fig. 7. Power profiles of PERC and HJT modules during a cloudy day.

for the first and second experimental campaign, respectively) for irradiance close to 1000 $\mathrm{W/m^2}$ and modules' temperature close to $70°C$. These results are currently valid for the period April - September in Italy after testing two PV modules per technology. In future works, longer experimental campaigns will be analyzed after testing a higher number of PV modules belonging to the same technology to increase the statistics of the analysis.

REFERENCES

[1] "Solar - iea." [Online]. Available: https://www.iea.org/energy-system/renewables/solar-pv

[2] A. Carullo, A. Ciocia, P. Di Leo, F. Giordano, G. Malgaroli, L. Peraga, F. Spertino, and A. Vallan, "Comparison of correction methods of wind speed for performance evaluation of wind turbines," *24th IMEKO TC4 International Symposium and 22nd International Workshop on ADC and DAC Modelling and Testing*, p. 291 – 296, 2020.

[3] A. Ciocia, P. D. Leo, S. Fichera, F. Giordano, G. Malgaroli, and F. Spertino, "A novel procedure to adjust the equivalent circuit parameters of photovoltaic modules under shading," *2020 International Symposium on Power Electronics, Electrical Drives, Automation and Motion, SPEEDAM 2020*, pp. 711–715, 6 2020.

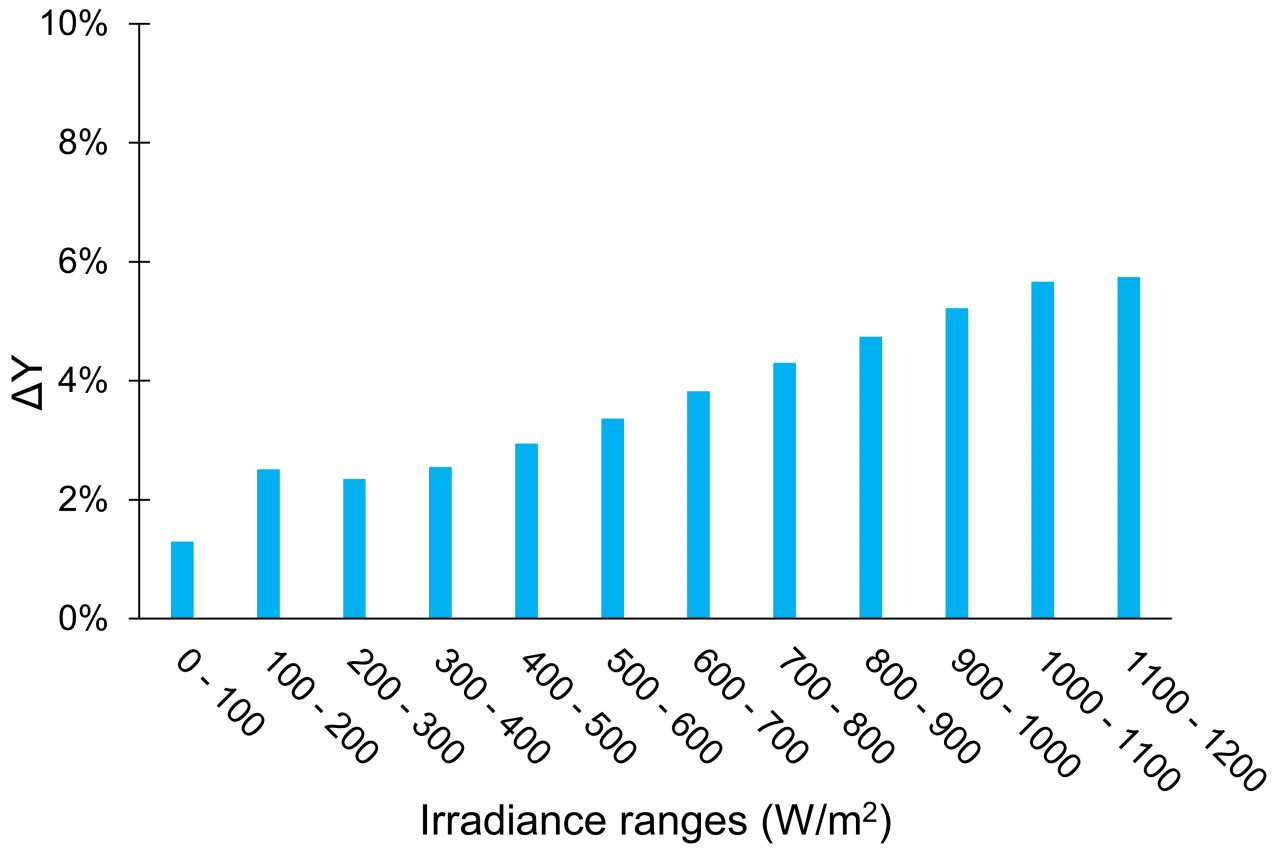

Fig. 8. Energy yield improvements over the irradiance ranges in the first campaign.

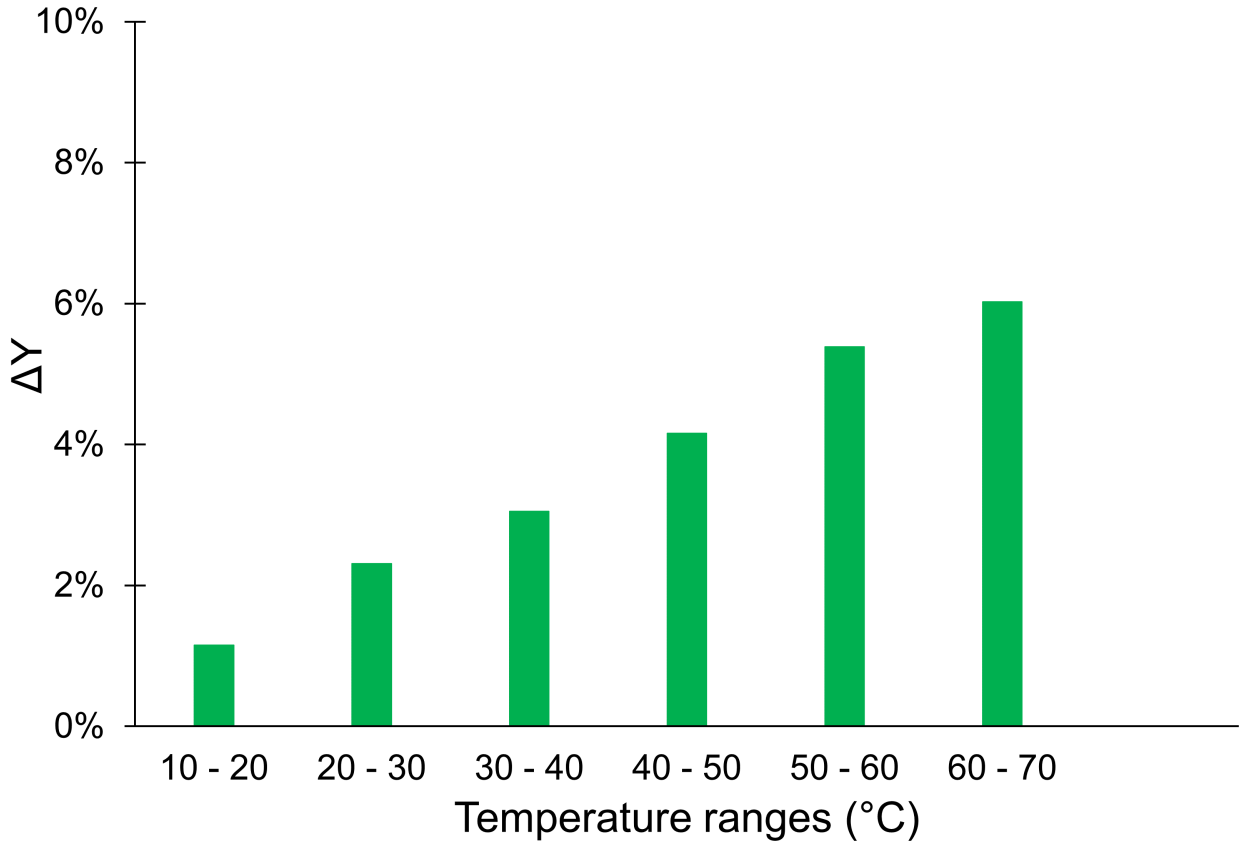

Fig. 9. Energy yield improvements over the modules' temperature ranges in the first campaign.

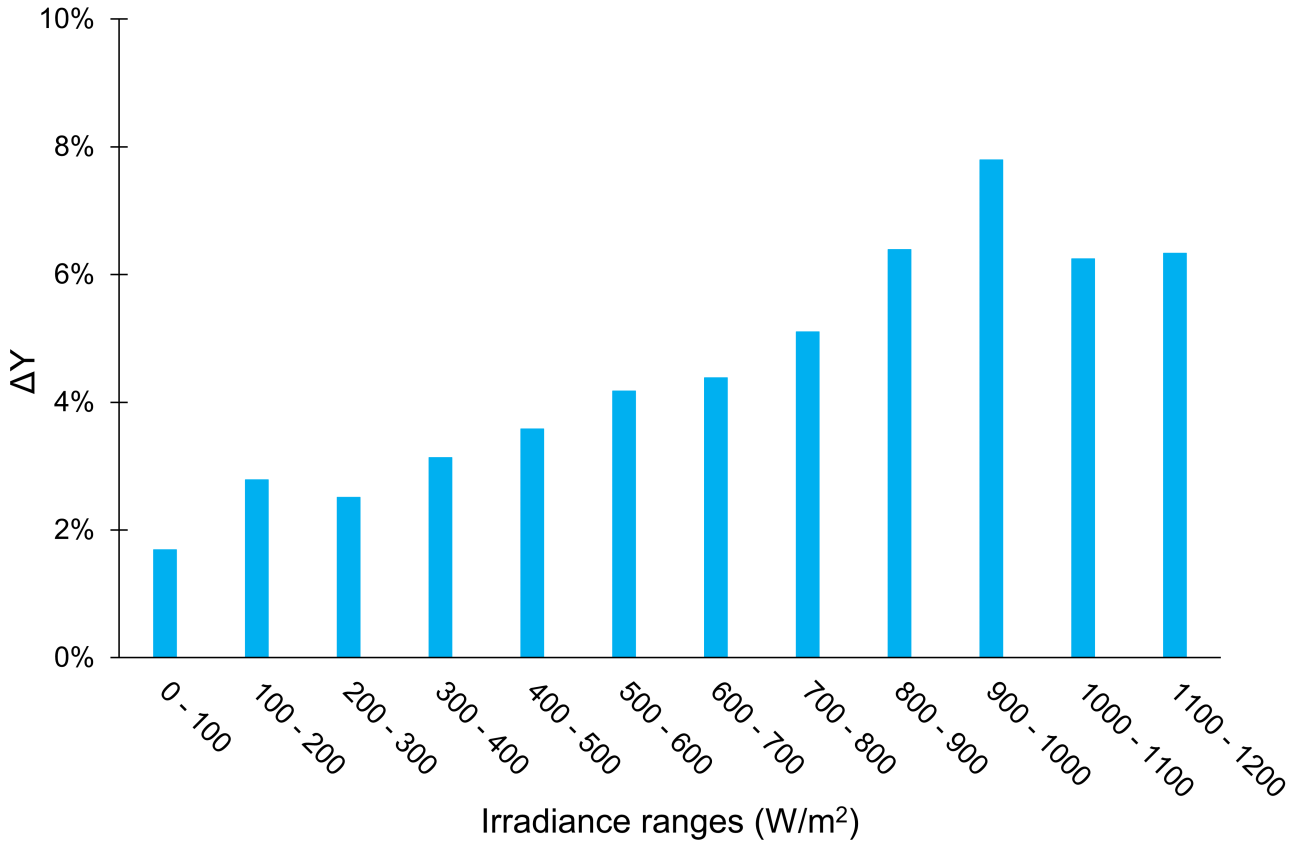

Fig. 10. Energy yield improvements over the irradiance ranges in the second campaign.

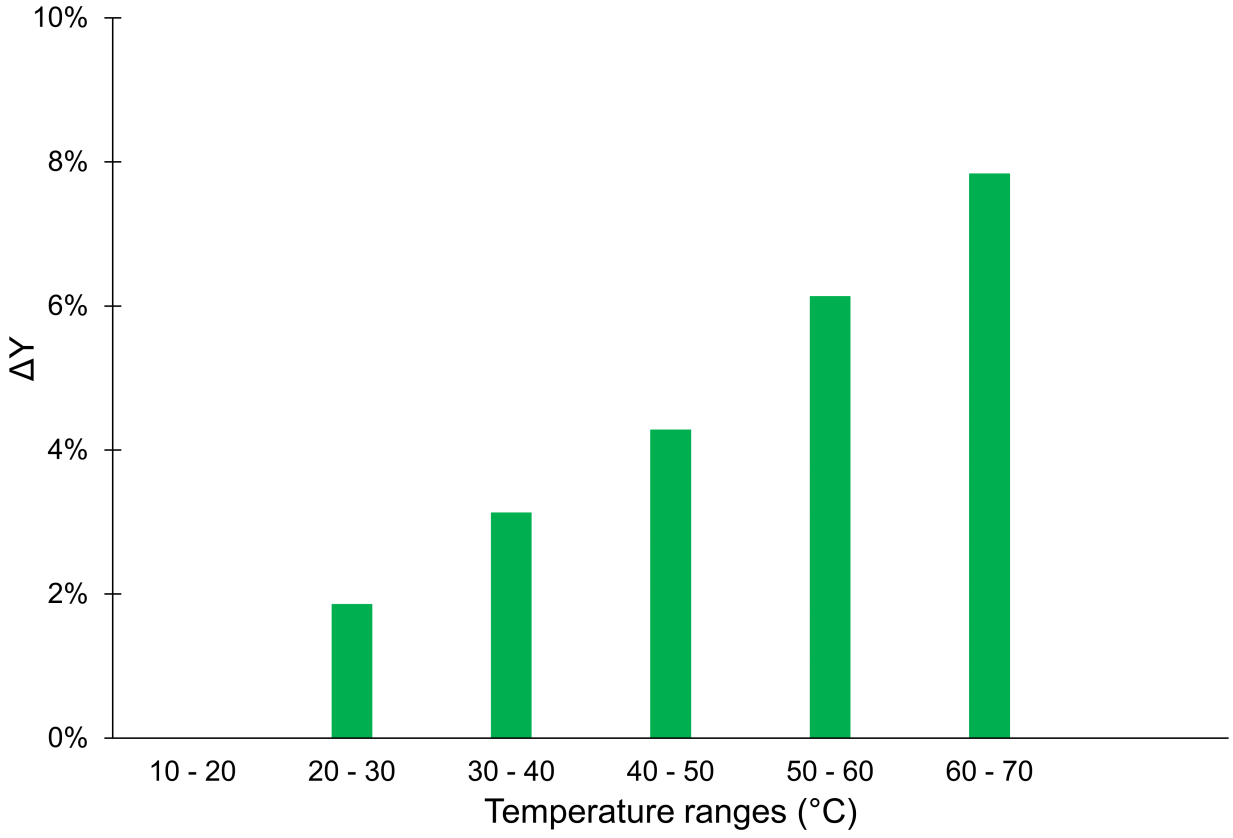

Fig. 11. Energy yield improvements over the modules' temperature ranges in the second campaign.

[4] G. Aime, A. Ciocia, G. Malgaroli, S. Narbey, L. Saglietti, and F. Spertino, "Degradation assessment for prototypal perovskite photovoltaic modules in long term outdoor experimental campaign," *Proceedings - 2023 IEEE International Conference on Environment and Electrical Engineering and 2023 IEEE Industrial and Commercial Power Systems Europe, EEEIC / I and CPS Europe 2023*, 2023.

[5] T. Fellmeth, S. Mack, J. Bartsch, D. Erath, U. Jäger, R. Preu, F. Clement, and D. Biro, "20.1% efficient silicon solar cell with aluminum back surface field," *Electron Device Letters, IEEE*, vol. 32, pp. 1101 – 1103, 09 2011.

[6] S. Kashyap, J. Madan, R. Pandey, and R. Sharma, "Comprehensive study on the recent development of perc solar cell," *Conference Record of the IEEE Photovoltaic Specialists Conference*, vol. 2020-June, pp. 2542–2546, 6 2020.

[7] J. Pastuszak and P. Wegierek, "Photovoltaic cell generations and current research directions for their development," *Materials*, vol. 15, 8 2022. [Online]. Available: /pmc/articles/PMC9414585/ /pmc/articles/PMC9414585/?report=abstract https://www.ncbi.nlm.nih.gov/pmc/articles/PMC9414585/

[8] "Top solar modules listing – may 2023 - taiyangnews." [Online]. Available: https://taiyangnews.info/top-solar-modules-listing-may-2023/

[9] "International technology roadmap for photovoltaic (itrpv) - vdma.org - vdma." [Online]. Available: https://www.vdma.org/international-technology-roadmap-photovoltaic

[10] N. Aste, C. D. Pero, and F. Leonforte, "Pv technologies performance comparison in temperate climates," *Solar Energy*, vol. 109, pp. 1–10, 11 2014.

[11] A. J. Carr and T. L. Pryor, "A comparison of the performance of different pv module types in temperate climates," *Solar Energy*, vol. 76, pp. 285–294, 1 2004.

[12] C. Cañete, J. Carretero, and M. S. de Cardona, "Energy performance of different photovoltaic module technologies under outdoor conditions," *Energy*, vol. 65, pp. 295–302, 2 2014.

[13] L. Wang, Y. Tang, S. Zhang, F. Wang, and J. Wang, "Energy yield analysis of different bifacial pv (photovoltaic) technologies: Topcon, hjt, perc in hainan," *Solar Energy*, vol. 238, pp. 258–263, 5 2022.

[14] H. Asav, G. Bektaş, A. E. Keçeci, G. Kökbudak, B. Arıkan, and R. Turan, "Comparative evaluation of rear local contact patterns for p-type mono crystalline silicon perc solar cell," *2020 2nd International Conference on Photovoltaic Science and Technologies (PVCon)*, pp. 1–4, 2020.

[15] "Trina solar sets 24th world record with 24.5% efficient 210 perc cell — trina solar." [Online]. Available: https://www.trinasolar.com/us/resources/newsroom/210-perc-cell-sets-world-record-24.5%25-efficiency

[16] Y. Liu, Y. Li, Y. Wu, G. Yang, L. Mazzarella, P. Procel-Moya, A. C. Tamboli, K. Weber, M. Boccard, O. Isabella, X. Yang, and B. Sun, "High-efficiency silicon heterojunction solar cells: Materials, devices and applications," 2020. [Online]. Available: https://doi.org/10.1016/j.mser.2020.100579

[17] P. magazine, "A closer look at longi's world record-breaking, 26.81%-efficient heterojunction solar cell," 2023. [Online]. Available: https://www.pv-magazine.com/2023/05/08/a-closer-look-at-longis-world-record-breaking-26-81-efficient-heterojunction-solar-cell/

[18] X. Fan, M. Rabelo, Y. Hu, Muhammad, Q. Khokhar, Y. Kim, and J. Yi, "Factors affecting the performance of hjt silicon solar cells in the intrinsic and emitter layers: A review," *Transactions on Electrical and Electronic Materials*, vol. 24, pp. 123–131, 2023. [Online]. Available: https://doi.org/10.1007/s42341-022-00427-3

[19] D. Bätzner, Y. Andrault, L. Andreetta, A. Büchel, W. Frammelsberger, C. Guerin, N. Holm, D. Lachenal, J. Meixenberger, P. Papet, B. Rau, B. Strahm, G. Wahli, and F. Wünsch, "Properties of high efficiency silicon heterojunction cells," *Energy Procedia*, vol. 8, pp. 153–159, 2011, proceedings of the SiliconPV 2011 Conference (1st International Conference on Crystalline Silicon Photovoltaics). [Online]. Available: https://www.sciencedirect.com/science/article/pii/S1876610211016262

[20] "Photovoltaic devices. procedures for temperature and irradiance corrections to measured i-v characteristics - bs en iec 60891:2021," Standard, Feb. 2022.

[21] "Photovoltaic module energy yield measurements: Existing approaches and best practice," report IEA-PVPS T13-11:2018.